Journal of Southeast University (English Edition) Vol. 35, No. 3, pp. 288 - 291 Sept. 2019 ISSN 1003—7985

Analytical models for circular and spherical dielectric elastomers

Zhang Hui Dai Min Zhang Zhisheng Xia Zhijie

(School of Mechanical Engineering, Southeast University, Nanjing 211189, China)

Abstract: In order to imitate skin characteristics, a dielectric elastomer (DE) membrane coated with flexible electrodes is applied with high voltage, which can lead to wrinkles and other phenomena. To develop soft-actuated air vehicles and other equipment, lightweight gas is pumped into a DE spherical shell to generate controllable flight movements. According to experimental phenomena and data, the calculation models of phase transitions on circular DE films are built. Meanwhile, the deformation characteristics of different DE (acrylic polymer and rubber) spherical actuators combined with helium are compared. The peak pressure inside a rubber balloon is greater than that of a VHB (acrylic polymer) balloon shell, but the limit stretch of rubber is much smaller. By taking advantages of this phenomenon, large deformations of a VHB spherical shell can be realized at an actuated state. Moreover, multi-layer spherical DE shells can achieve larger voltage-induced volume change than monolayer ones. The research indicates that pre-stretching is one of the key factors to induce phase transitions between flat, wrinkled and bulging regions on circular DE films, and the internal pressure determines the electromechanical performance of balloon actuators.

Key words: dielectric elastomer; circular frame; balloon actuator; large deformation; phase transition

DOI: 10.3969/j.issn.1003-7985.2019.03.003

Soft active materials are utilized to manufacture soft machines, and they emerge as an exciting engineering field. Dielectric elastomer actuators (DEAs) are a kind of soft active materials which can deform in response to voltage[1-2], and they are used in a variety of innovative applications, such as medical devices[3], and unmanned flight systems[4], etc. Suitably designed DEAs usually cause giant voltage-induced deformation and beauty phase transitions prior to electric breakdown[5]. Yu et al.[6] studied the propagation of wrinkles in dielectric elastomers after observing the skin and feet of animals. Huang and Suo[7] theoretically analyzed the transition in DE membranes under uniaxial loads. Lu and Suo[8] studied the electromechanical phase transition between bulged and unbulged states in a dielectric tube. Recently, Godaba et al.[9] observed wrinkle patterns in DE membranes, and the flat and wrinkled regions coexisted.

Recently, DEAs coupled with electrodes and lighter gas have been developed as soft pumps and robots. Zhu et al.[10] studied a thin-walled DE balloon and analyzed its nonlinear oscillation. Chen et al.[11] analyzed the dynamic performance of DE balloon actuators driven by a pressure and a voltage. Zhang et al.[12] presented balloon actuators based on DEs, and the initial volume was important for large deformation.

This paper investigates analytical models for circular DE membranes, and studies dynamic patterns on their surfaces. The performance of DE balloon actuators coupled with helium gas is also proposed, and the mass change can be controlled for application in soft-actuated air vehicles. The purpose of this research is to optimize the parameters and theoretical models of DEs, and to give some guidelines for intelligent soft robots and devices.

1 Equations for Deformation

Fig. 1 illustrates the experimental setup for observing the phase transitions on a circular DE film. Voltage is programmed with the software of Labview and amplified by a high voltage amplifier (10/40 A). Cameras are employed to capture the side view of DE actuators. A circular membrane is axisymmetric in its configuration, as shown in Fig. 1, consisting of an active region with electrodes and a passive part. The voltage is then applied to the active region which expands into a new state of equilibrium. In the case of the pre-stretch $\lambda_{pre} = 1$, the volt-

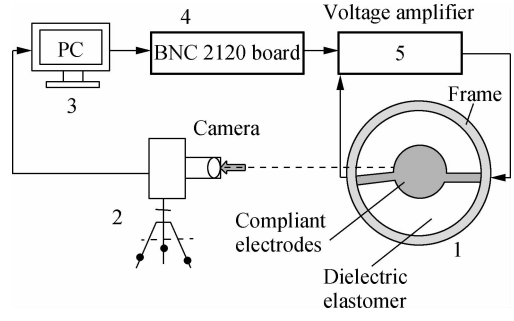

1— Circular DE actuator; 2— Camera to take pictures and videos of the side view; 3—Computer; 4—BNC 2120 junction box; 5—High voltage amplifier

Fig. 1 Experimental setup for a circular DE membrane

Received 2018-12-09, **Revised** 2019-04-11.

Biographies: Zhang Hui (1987—), female, doctor, assistant researcher; Zhang Zhisheng (corresponding author), male, doctor, professor, oldbc@seu.edu.cn.

Foundation item: The National Natural Science Foundation of China (No. 51775108).

Citation: Zhang Hui, Dai Min, Zhang Zhisheng, et al. Analytical models for circular and spherical dielectric elastomers[J]. Journal of Southeast University (English Edition), 2019, 35(3): 288 - 291. DOI: 10.3969/j.issn.1003-7985.2019.03.003.

age will induce compressive stresses in the passive region, and the thin membrane can experience out-of-plane bulging due to the loss of tension (LT).

In the actuated state, the circular active part undergoes homogeneous, equal-biaxial deformation, which is different from the passive region. λ_r and λ_θ are the stretches in the radial and hoop directions, respectively. Using geometry, $\partial\lambda_\theta/\partial R = \lambda_r/R - \lambda_\theta/R$. R is the reference radius of an arbitrary point in the active region, and r is the deformed radius of the same particle during the actuated state.

The element in a circular DE membrane undergoes tri-axial stresses σ_r, σ_φ and σ_θ which correspond to nominal stresses S_r, S_φ and S_θ, respectively. Mechanical equilibrium requires that $\partial\sigma_r/\partial r = (\sigma_\theta - \sigma_r)/r$. Therefore, the state equation can be written as a sum of two parts $\lambda_\theta S_\theta + ED = \lambda_\theta \dfrac{\mathrm{d}W}{\mathrm{d}\lambda_\theta}$, where E is the electric field, and W represents the Helmholtz free energy density of the DE material. The electric displacement D is linear, and it satisfies $D = E\varepsilon$. ε is the permittivity. When we set $ED = 0$, the stresses can be expressed by $\sigma_r = \lambda_r \dfrac{\mathrm{d}W}{\mathrm{d}\lambda_r}$, $\sigma_\theta = \lambda_\theta \dfrac{\mathrm{d}W}{\mathrm{d}\lambda_\theta}$. Once the hoop stretch at the inner boundary is known, the hoop stress, namely $S_\theta = \dfrac{\mathrm{d}W}{\mathrm{d}\lambda_\theta}$, can be calculated. Then, we obtain $\sigma_\theta = \lambda_\theta S_\theta$. When $S_\theta = 0$, the loss of tension that induces phase transitions is apparent.

The state of the active part is governed by $ED = \lambda_\theta \dfrac{\mathrm{d}W}{\mathrm{d}\lambda_\theta}$ under the LT condition. The inner boundary is at the interface between the active region and passive region on a DE membrane, and the outer boundary is the rigid frame. The voltage Φ is applied to the active part. Due to the unchanged volume, $\dfrac{\lambda_\theta - \lambda_\theta^{-5}}{(J_{\lim}+3)\lambda_\theta^3 - 2\lambda_\theta^5 - \lambda_\theta^{-1}} = \dfrac{\varepsilon\Phi^2}{\mu H^2 J_{\lim}}$.

The stretch ratio of the radius is λ_i, namely $\lambda_i = r_{i+1}/r_i$. The function related to λ_i and λ_{pre} is expressed by

$$f(\lambda_{\mathrm{pre}}, \lambda_i) = \frac{2\lambda_{\mathrm{pre}} - \lambda_i}{2\lambda_i - \lambda_{\mathrm{pre}}} \frac{\partial W}{\partial \lambda_{\mathrm{pre}}} \tag{1}$$

The relationship between the voltage and the stretch is given. Furthermore, the dielectric breakdown voltage is calculated by $\Phi_{\mathrm{DB}} = 35.6H\lambda_\theta^{-0.87}$.

$$\frac{\partial W}{\partial \lambda_i} - f(\lambda_{\mathrm{pre}}, \lambda_i) = \frac{\varepsilon\Phi^2}{H^2}\lambda_i^3 \tag{2}$$

Fig. 2(a) presents a spherical DE membrane with the original radius R and thickness H. It consists of monolayer elastomer (VHB or natural rubber), and carbon grease is smeared on the exterior and interior surfaces of the spherical membrane to serve as electrodes. Inner initial pressure p_0 is equal to the atmospheric pressure. The gas is pumped into the balloon, and then the actuator is sealed. Consequently, the actuator is subject to pressure

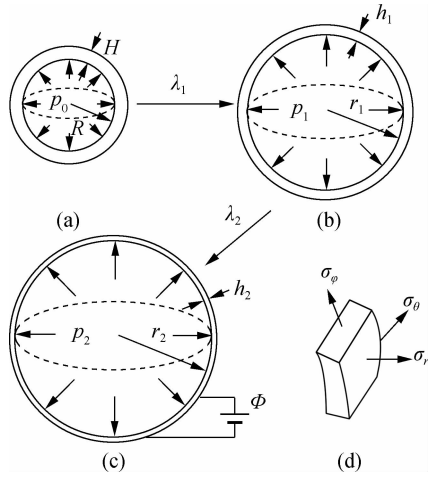

Fig. 2 Schematic of a DE spherical shell. (a) Original state; (b) Pre-stretched state; (c) Actuation state; (d) Deformed state of the element in a DE film subjected to tri-axial stresses

p_1, and the radius and thickness become r_1 and h_1, respectively, as shown in Fig. 2(b). Fig. 2(c) shows that the balloon deforms to an equilibrium state with radius r_2 and thickness h_2 corresponding to current pressure p_2 and voltage Φ. In Fig. 2(d), we define $\sigma_\theta = \sigma_\varphi = p\dfrac{r}{2h}$, $\sigma_r = 0$.

In Fig. 2, from states (a) to (c), thermodynamics dictates that the arbitrary variation of free energy in a DE membrane should equal the work done by the voltage, pressure and inertia, so that $\dfrac{\delta W}{\delta r} = \dfrac{2\Phi D\lambda}{RH} + \dfrac{P}{H}\lambda^2 - \rho\dfrac{\mathrm{d}^2 r}{\mathrm{d}t^2}$. The DE balloon actuator consists of two independent variables (λ and D). Combined with the free-energy function, there is $\dfrac{\partial W}{\partial \lambda} = \dfrac{2\Phi D\lambda}{H} + \dfrac{PR}{H}\lambda^2 - R^2\rho\dfrac{\mathrm{d}^2\lambda}{\mathrm{d}t^2}$.

From Figs. 2(a) and (b), the stretch ratio in the gas pumping process is prescribed as $\lambda_1 = r_1/R$, $\lambda_1^3 = 3V_1/(4\pi R^3)$, and V_1 is the volume. The pressure in the balloon is

$$p_1(\lambda_1) = \frac{4H}{R\lambda_1^2}\frac{\partial W}{\partial \lambda_1} \tag{3}$$

The fixed amount of gas is enclosed. Combining the ideal gas law, the internal pressure of a DE balloon actuator is

$$p_i(\lambda_1, \lambda) = \frac{p_1 + p_{\mathrm{atm}}}{\lambda^3 - p_{\mathrm{atm}}}\lambda_1^3 \tag{4}$$

Then, the pressure decreases with the increase in the volume caused by the voltage, and it is described as

$$\frac{p_i R}{4H}\lambda^2 = \frac{\mathrm{d}W}{\mathrm{d}\lambda} - \frac{\varepsilon\Phi^2}{2H^2}\lambda^3 \tag{5}$$

The condition of dielectric breakdown is expressed[13] as $E_{\mathrm{DB}} = 30.6\lambda^{1.13} \times 10^6$. The voltage corresponding to

E_{DB} is $\Phi_{DB} = E_{DB} H\lambda^{-2}$.

Fig. 3 shows that DE balloon actuators are characterized by the desired nonlinear pressure-prestretch relationship $\lambda_1 = r_1/R$. The curves follow the trends predicted by analytical models. The original radius R is 3.50, 7.25 and 12.75 cm, respectively. In Fig. 3(a), the stretch limit $J_{lim} = 175$ and shear modulus $\mu = 35$ kPa are used. Electric breakdown always occurs at about Φ = 6 kV. From Fig. 3(b), the parameters $\mu = 350$ kPa, and $J_{lim} = 35$. Electric breakdown commonly occurs at about $\Phi = 3$ kV. The original thicknesses of the rubbers are chosen to be 0.25, 0.4 and 0.47 mm, respectively. It is found that the peak pressure in a rubber balloon is greater than that of a VHB spherical shell. The limit stretch of natural rubber is much smaller than that of the VHB material.

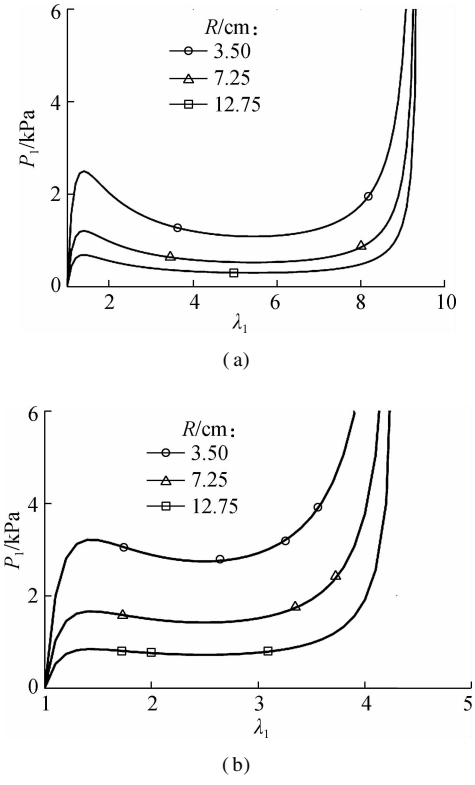

Fig. 3 Pressure p_1 in gas pumping process as a function of pre-stretch λ_1. (a) Pressure change in VHB 4910 balloon shells; (b) Pressure change in natural rubber balloons

Fig. 4 plots the gas law for numbers of molecules within a rubber balloon and a VHB balloon, respectively. The rhombus curve represents the number of gas moles in a rubber balloon, and the dotted line shows that in a VHB 4910 spherical shell. With the same original diameter (7 cm) and pre-stretch, the initial thickness of VHB membrane is 1 mm, for rubber it is 0.25 mm. As a result, the gas amount in the rubber balloon is more than that in the VHB balloon, because VHB is a softer material.

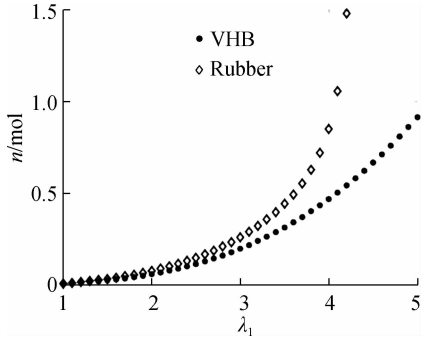

Fig. 4 Relationship between the number of gas moles and pre-stretch

2 Discussion

Phase transitions are observed on circular DE membranes (the original thickness H = 1 mm) with different pre-stretch λ_{pre}. In the pre-stressed state, thin membranes are flat, as shown in Fig. 5(a) and Fig. 6(a). When the voltage is relatively small, the membrane keeps flat and elongates around the frame. As the voltage further increases, the tensile stress in the passive region decreases gradually. At a critical voltage, bulging (see Fig. 5(c), λ_{pre} = 1) or wrinkles (see Fig. 6(c), λ_{pre} = 4) appears. Wrinkled regions can spread over the entire membrane within a short time.

Fig. 5 The phase transition from the flat state to bulging state under different voltages. (a) 0 kV; (b) 7 kV; (c) 9.5 kV

Fig. 6 The phase transition from the flat state to wrinkle state under different voltages. (a) 0 kV; (b) 5.5 kV; (c) 6.6 kV

For DE balloons, when the voltage is applied to double-layer spherical membranes, the volume change is larger than that of monolayer DE balloons. A new method is also used to obtain a large deformation of a DE balloon. After dielectric breakdown of the inner rubber, we continue to apply the voltage to the double-layer spherical VHB membranes and the balloon further expands its volume without gas leakage. This process can increase the mass change and it is controlled in the flight robot system[14].

3 Conclusions

1) This paper investigates the calculation models for

the analysis of circular and spherical DE membranes. Phase transitions among flat, bulging and wrinkles can be theoretically predicted and experimentally observed in a narrow voltage range prior to electrical failure.

2) The analytic models of soft balloon actuators combining free energy and the ideal gas law can provide guidance for experiments. Larger deformations of multi-layer DE balloons are also explored. The spherical DE membranes can be utilized in a giant deformation to produce the controlling force, and they have potential application for soft flight robots.

3) It is hoped that the proposed theory and results will help the design of DEAs and maximize their actuation performance.

References

[1] Zhang H, Zhang Z S. Phase transitions of dielectric elastomers in a circular frame [J]. *Journal of Southeast University (English Edition)*, 2017, **33**(4): 387 - 390. DOI: 10.3969/ j. issn. 1003-7985. 2017. 04. 001.

[2] Wu J F, Li J Q, Song A G, et al. Electrostrictive properties on polyurethane elastomers [J]. *Journal of Southeast University(Natural Science Edition)*, 2008, **38**(3): 439 - 443. DOI: 10. 3321/j. issn: 1001 - 0505. 2008. 03. 015. (in Chinese)

[3] Roche E T, Wohlfarth R, Overvelde J T B, et al. A bioinspired soft actuated material [J]. *Advanced Materials*, 2014, **26**(8): 1200 - 1206. DOI: 10. 1002/adma. 201304018.

[4] Zhang H, Zhou Y F, Dai M, et al. A novel flying robot system driven by dielectric elastomer balloon actuators [J]. *Journal of Intelligent Material Systems and Structures*, 2018, **29** (11): 2522 - 2527. DOI: 10. 1177/1045389x18770879.

[5] Mao G Y, Huang X Q, Diab M, et al. Controlling wrinkles on the surface of a dielectric elastomer balloon [J]. *Extreme Mechanics Letters*, 2016, **9**: 139 - 146. DOI: 10. 1016/j. eml. 2016. 06. 001.

[6] Yu J, Chary S, Das S, et al. Gecko-inspired dry adhesive for robotic applications [J]. *Advanced Functional Materials*, 2011, **21**(16): 3010 - 3018. DOI: 10. 1002/adfm. 201100493.

[7] Huang R, Suo Z G. Electromechanical phase transition in dielectric elastomers [J]. *Proceedings of the Royal Society A: Mathematical, Physical and Engineering Sciences*, 2012, **468** (2140): 1014 - 1040. DOI: 10. 1098/rspa. 2011. 0452.

[8] Lu T Q, Suo Z G. Large conversion of energy in dielectric elastomers by electromechanical phase transition [J]. *Acta Mechanica Sinica*, 2012, **28**(4): 1106 - 1114. DOI: 10. 1007/s10409-012-0091-x.

[9] Godaba H, Zhang Z Q, Gupta U, et al. Dynamic pattern of wrinkles in a dielectric elastomer [J]. *Soft Matter*, 2017, **13**(16): 2942 - 2951. DOI: 10. 1039/c7sm00198c.

[10] Zhu J, Cai S Q, Suo Z G. Nonlinear oscillation of a dielectric elastomer balloon [J]. *Polymer International*, 2010, **59**(3): 378 - 383. DOI: 10. 1002/pi. 2767.

[11] Chen F F, Wang M Y. Dynamic performance of a dielectric elastomer balloon actuator [J]. *Meccanica*, 2015, **50** (11): 2731 - 2739. DOI: 10. 1007/s11012-015-0206-0.

[12] Zhang H, Wang Y X, Zhu J, et al. Balloon actuators based on the dielectric elastomer [C]//*IEEE International Conference on Industrial Technology*. Toronto, Canada, 2017: 654 - 658. DOI: 10. 1109/icit. 2017. 7915436.

[13] Koh S J A, Keplinger C, Li T F, et al. Dielectric elastomer generators: How much energy can be converted? [J]. *ASME Transactions on Mechatronics*, 2011, **16**(1): 33 - 41. DOI: 10. 1109/tmech. 2010. 2089635.

[14] Zhang H, Wang Y X, Godaba H, et al. Harnessing dielectric breakdown of dielectric elastomer to achieve large actuation [J]. *Journal of Applied Mechanics*, 2017, **84** (12): 121011. DOI: 10. 1115/1. 4038174.

圆形和球形结构介电弹性体的解析模型

张 慧 戴 敏 张志胜 夏志杰

(东南大学机械工程学院,南京 211189)

摘要:为了模仿皮肤特征,对涂有柔性电极的介电弹性体(DE)膜施加高电压,使其产生纹理褶皱等现象. 为了开发软驱动飞行器等设备,往 DE 球壳内部充入质轻气体,使其产生可控的飞行运动. 依据实验现象与数据,建立了圆形 DE 薄膜相变转换的计算模型;同时,比较了不同的 DE (丙烯酸聚合物和乳胶) 球体驱动器与氦气相结合的变形特征. 乳胶气球内部的压力峰值远大于 VHB(丙烯酸聚合物)球体的压力峰值,但是其极限拉伸却较小,利用这一现象,能够实现 VHB 球壳在驱动状态下的大变形. 另外,多层 DE 球形壳在电压作用下,能够实现比单层球壳更大的体积变化. 研究表明:预拉伸是引起圆形 DE 膜平坦、皱褶和膨胀区域之间相变转换的关键因素之一;内部压强决定着球体驱动器的机电性能.

关键词:介电弹性体; 圆形框架; 球体驱动器; 大变形; 相变转换

中图分类号:TH134